Power Electronics and Drives
Volume 9(44), 2024 DOI: 10.2478/pead-2024-0001

Power Electronics and Drives

Enhancing PV Systems with Intelligent MPPT and Improved control strategy of Z-Source Inverter

Research paper

Fares Bettahar*, Abdeddaim Sabrina, Betka Achour

LGEB, University of Mohamed Khidar, Biskra, Algeria

Received: 28 July, 2023; Accepted: 13 October, 2023

Abstract: The Improved Z-Source Inverter (IZSI) has gained attention in the photovoltaic industry for its ability to boost PV voltage with a single-stage topology, simplifying system design and reducing costs. However, research on integrating IZSI into PV systems, particularly regarding the Maximum Power Point Tracker (MPPT) and IZSI control strategy, is limited. This study proposes an Intelligent Improved Particle Swarm Optimization (IPSO) algorithm as an MPPT method for PV systems under constant and varying irradiance conditions. The IPSO algorithm is compared to the FPA, CSA, and traditional MPPT algorithm (PSO), and the results demonstrate that IPSO outperforms all algorithms in terms of speed, efficiency, and convergence in finding the Maximum Power Point (MPP). Two methods, Simple Boost Control (SBC) and Maximum Constant Boost Control with Third Harmonic Injection (THIMCBC), are employed to control IZSI. Simulation results using MATLAB-Simulink show that both strategies successfully find and track the MPP, but THIMCBC exhibits superior voltage-boosting performance compared to SBC. Overall, the proposed IZSI topology with the IPSO MPPT method and THIMCBC IZSI control strategy offers several advantages, including improved voltage boost ability, reduced z-source capacitor voltage stress, inherent inrush current limitation, and cost-effectiveness. These advantages make the proposed system a promising solution for photovoltaic systems.

Keywords: *Photovoltaic Systems • improved ZSI • IPSO • THIMCBC*

1. Introduction

The search for new energy sources has received significant attention as the energy crisis and environmental pollution worsen. The photovoltaic (PV) system has become increasingly promising as a source of renewable energy (Peng, Bo-Ruei et al., 2018). Operating the photovoltaic (PV) system at its maximum power point (MPP) offers significant advantages, including cost minimization and enhanced efficiency. However, the process to extract the maximum power can be difficult because the PV panel current and voltage have a non-linear relationship (Jayaudhaya, J. et al., 2022).

Hence, in the quest to achieve the maximum power point (MPP) for photovoltaic (PV) systems, the utilization of maximum power point tracking (MPPT) techniques is prevalent. The effectiveness of Perturb and Observe (P&O) (Ali, Ahmed Ismail M. et.al 2022) and Incremental Conductance (IC) (Anto, Emmanuel Kwaku et al., 2014), methods for Maximum Power Point Tracking (MPPT) in photovoltaic (PV) systems may vary depending on specific environmental conditions and system characteristics. While these conventional methods have been widely used due to their simplicity, some studies have identified limitations, such as oscillations and slow convergence, particularly under rapidly changing or challenging. As a result, more advanced MPPT techniques have been developed to address these issues and improve overall performance.

* *Email: fares.bettahar@univ-biskra.dz*

Metaheuristic methods are the focus of research because they perform better. To name a few GA (Balasubramanian, Ashok et al., 2022), GWO (Mahapatra, Sadhan and Chandan Kumar Sah.), BAT (Tey, Kok Soon et al., 2018), CS (Chauhan, Urvashi et al., 2018) and FPA (Luthfansyah, Mohammad et al., 2020).

A photovoltaic system made up of numerous PV modules needs to be able to produce enough output voltage before it can be connected to a load or the grid (Hanafiah, Stefan et al., 2017). When facing issues with insufficient PV output voltage, engineers commonly resort to traditional two-stage inverters DC/DC DC/AC. However, this approach necessitates the addition of a second DC-DC boost converter, escalating controller complexity, diminishing overall efficiency, and inflating inverter costs.

To address this challenge, Z-source inverters have gained importance in modern power electronics due to their various topologies and unique characteristics. ZSI mainly focuses on increasing voltage and achieving single-stage DC-AC conversion (Subhani, N, Kannan et al. 2021). The design includes an impedance source network in an X-shaped configuration consisting of two capacitors and two inductors connected to the DC input source. In contrast to conventional traditional voltage source inverters. However, this proposed topology Z-source has some disadvantages, such as: large voltage stress across the switches and capacitors, a huge inrush current and a small boost factor.

Recent research on Z-source inverters (ZSI) has shown that there is a focus on modulation strategies field applications and inverter modelling in (Jamal I., Elmorshedy et al., 2022). Although these evolving topologies offer significant advantages they are not without limitations, particularly high costs and potential damage due to current surges and resonances on Z-inductors and Z-capacitors. This research focuses on the form of an Improved ZSI topology that is strategically designed to overcome the limitations of traditional ZSI by optimizing voltage boosting and control strategies.

In addition to its technical advantages, the Improved Z-Source Inverter (IZSI) offers a significant physical advantage. The IZSI achieves cost parity with the traditional Z-Source Inverter using identical components. The main distinguishing feature is the thoughtful rearrangement and positioning of these components within the topology. This nuanced yet strategic alteration bestows a substantial technical advantage upon the IZSI over the ZSI enhancing efficiency (Amudhavalli and Narendran in 2012), reducing voltage stress and improving surge control without imposing an economic burden. Structural enhancements often incur a notable financial cost due to increased components. This study shifts its focus towards the control aspect, specifically optimizing the extraction of maximum energy from a solar panel and augmenting boosting voltage through control strategies. The IZSI prioritizes heightened efficiency without inflating costs and maintains cost parity with the traditional Z-Source Inverter (ZSI). Striking this balance ensures a technical advantage in performance, efficiency and cost.

This work focuses on integrating the improved ZSI into the PV system using the MBC and THIMCBC control method to improve voltage boosting with the following MPPT algorithms: PSO, CSA, FPA and IPSO. The first section of this paper explains the overall system design that includes the PV system and IZSI with a comparative study of both ZSI topologies. The following section then provides a brief description of the PV modules and MPPTs algorithms used. The third section explains the enhanced Z-source inverter (IZSI) and control strategies. Finally, the simulation results are based on the Matlab /Simulink software and a comparative study is presented.

2. Global System Design

As shown in Figure 1, the photovoltaic (PV) system studied in this work consists of a PV module, single phase capacitor voltage, improved Z-source inverter, IPSO as MPPT with THIMCBC control, filtering the output voltage of three-phase system using LC filter, and resistive three phase R load. The MPPT control algorithm decides how to move the PV module's operating voltage by adjusting the duty cycle directly responsible for controlling the improved-Z source inverter.

2.1. Solar PV System

Photovoltaic (PV) systems are the conversion of light into electricity using semiconductor materials that exhibit the photovoltaic effect. The cell model is important in solar PV system modelling because the accuracy of cell characteristics is what determines system performance. A one-diode circuit model was used to predict cell characteristics (Hayder, Wafa et al., 2020). Figure 2 represents the electrical behavior of a PV cell because commonly accepted solar cell model and to avoid complexity.

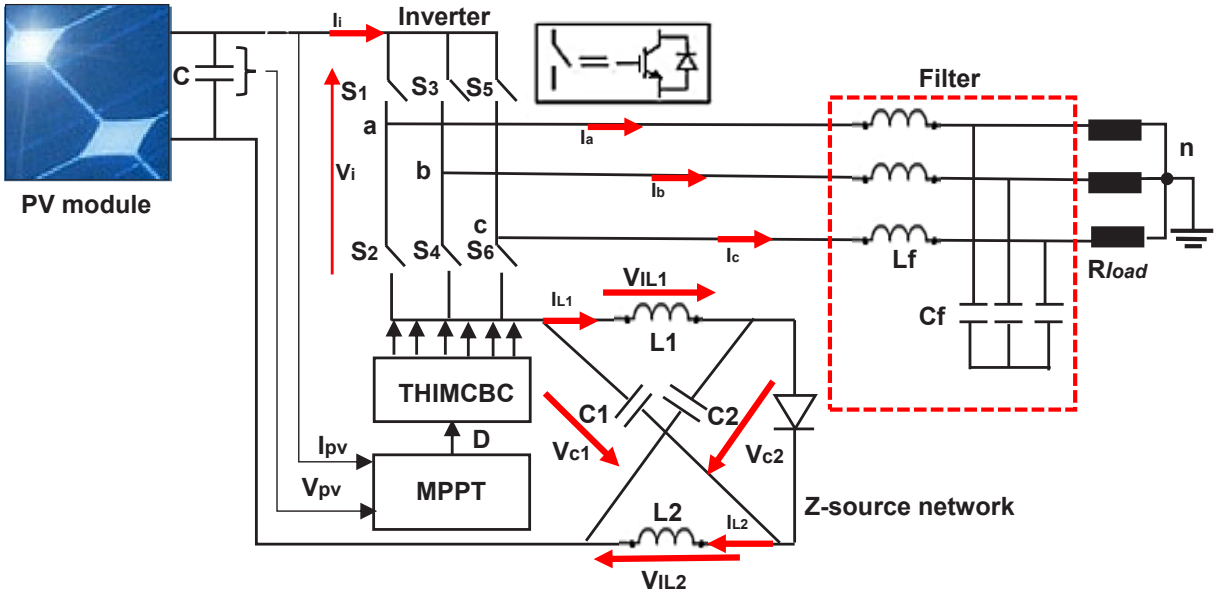

Fig. 1. Improved -Z-source inverter with LC filter in PV application.

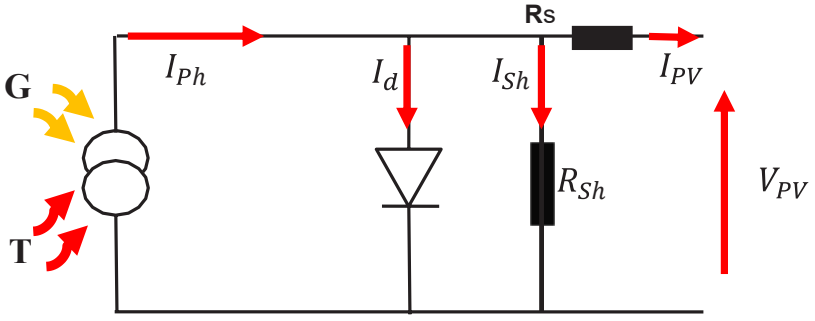

Fig. 2. Model of a photovoltaic cell.

By using Kirchhoff's current law (KCL), mathematical equations of this model are the following (Ibtissam, Chaib et al 2018).

$$I_{pv} = I_{ph} - I_d - I_{sh} \tag{1}$$

$$I_{pv} = I_{ph} - I_S\left[\exp\left(\frac{V + IR_s}{nV_T}\right) - 1\right] - \left[\frac{V + IR_s}{R_{sh}}\right] \tag{2}$$

$$I_{ph} = \left[I_{scr} + K_i\left(T_c - T_{ref}\right)\right]\frac{G}{G_{ref}} \tag{3}$$

Where: IScr : solar cell short-circuit current, Gref : reference solar insolation in W/m^2,Tref : cell reference temperature, Ki : cell short-circuit current temperature coefficient, G : solar insolation in W/m^2. On the other hand, the cell saturation current varies with the cell temperature, which is described as:

$$I_S = I_0\left(\frac{T_c}{T_{\text{ref}}}\right)^3 \exp\left[\frac{qE_g}{nk}\left(\frac{1}{T_{\text{ref}}} - \frac{1}{T_c}\right)\right] \tag{4}$$

Where: I0: cell reverse saturation current at standard condition (T=25 ^{0}C, G=1000W/m^2), Eg: band-gap energy of the Si solar cell, where Eg=1.1eV and n: is the series cell number. The reverse saturation current at reference temperature can be approximately obtained as:

$$I_0 = \frac{I_{sc}}{exp\left(\frac{qV_{oc}}{nkT_c}\right) - 1} \tag{5}$$

In this work, which consists of two series modules connected in parallel with another two series modules (2S2P configuration). The module delivers a maximum power output equal to 175 W at standard temperature condition (STC).The electrical parameters of this module is listed in Table 1.

After being connected, the characteristic current to voltage I(V) and power to voltage P(V) of the entire system were extracted under various solar radiation influences (400,600,800, and 1000W/m^2) at the same surface temperature of 25 °C. This was done as a non-linear test, where one point stood in for the maximum power, or "MPP" then keep an eye on the impact on the P (V), I (V). Similar results with temperature changes of 25, 40, 50 and 65°C at constant solar radiation (1000 W/m^2).

The power generated by photovoltaic (PV) systems is influenced by solar radiation. An increase in solar radiation results in an increased power output, as depicted in Figure 3(a). However, the relationship is not a simple direct proportionality. On the other hand, an increase in temperature leads to a decrease in voltage, which in turn lowers the power output, even with stable current values, as illustrated in Figure 3(b).

Parameters	Variable	Value
Short circuit current	I_{sc}	5.4 A
Open circuit voltage	V_{oc}	44 V
Current of P_{max}	I_{MPP}	4.95 A
Voltage of P_{max}	V_{MPP}	35.4 V
Maximum power	P_{MPP}	175 W
series resistance	R_s	0.5 Ω
I_{sc} *coaf*. of temperature	K_i	0.0013A/°C

Table 1. Specification of the solar panel.

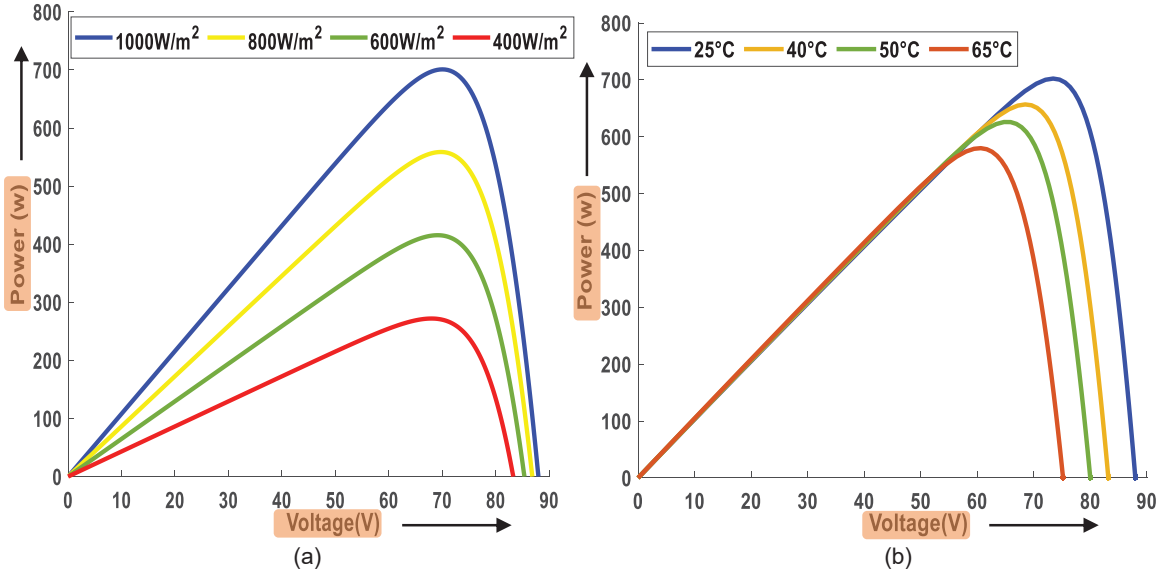

Fig. 3. (a) P–V Characteristics for different Irradiation levels for Constant Temperature (b) P–V and characteristics for different Tempera true Levels and Constant Irradiance.

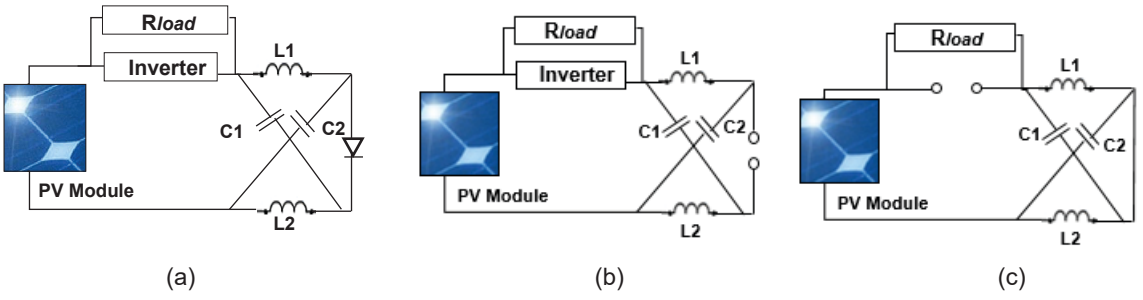

Fig. 4. (a) Simplified equivalent circuit of improved ZSI (b) Shoot-through state (c) Non shoot-through state.

2.2. Improved Z-Source Inverter

The Improved Z-Source Inverter (IZSI) depicted in (a) Figure 4, as described in (Jagan, Vadthya and Sharmili Das 2015), employs a similar set of components as the traditional inverter, with one key difference. Specifically, in the IZSI topology, the placement of the Inverter Bridge and diode are switched, and their connection direction is reversed compared to the traditional topology. This means that in the traditional topology, the inverter bridge is connected in parallel with the Z-source, whereas in the IZSI, the inverter bridge is connected in series with the Z-source network. The IZSI was developed to address some of the drawbacks associated with the conventional ZSI, such as the need to avoid voltage stress across the capacitors, suppress high inrush current, and reduce resonance between inductors and capacitors during startup.

(Yu, Kun et al 2010) explain two modes of the improved Z-source inverter. The shoot-through state involves closing switches simultaneously on the same phase leg of the inverter, resulting in a reverse-biased diode and short-circuited inductive load. The non-shoot-through state allows the inverter to operate in active or null states, similar to a traditional VSI, with a forward-biased diode. These modes offer flexibility and improved performance compared to traditional VSIs.

The operational principle (Tang. Y, Xie et al.,2011) depicted in Figure 4 illustrates the equivalent circuit for IZSI. When $L = L_1 = L_2$ and $C = C_1 = C_2$, the voltages across inductors and capacitors are identical. In the shoot-through state (Figure 4(b)), the inverter side is shorted, resulting $V_L = V_{pv} + V_c$. In the non-shoot-through state (Figure 4(c)), the inductor voltage is given by:

$$V_L = -V_c \tag{6}$$

The duty ratio during the shoot-through state is *D*, and over one switching period, the average V_L is zero, expressed as:

$$V_c = \frac{D}{1-2D} V_{pv} \tag{7}$$

In this state, the Z-source capacitor voltage V_c is zero when *D* is zero. The peak DC-link voltage V_i and peak output phase voltage V_{an} can be expressed as:

$$V_i = V_{pv} + 2V_c = \frac{1}{1-2D} V_{pv} = Bv_{pv} \tag{8}$$

$$V_{an} = \frac{MV_{inv}}{2} = \frac{MBV_{pv}}{2} \tag{9}$$

Where *B* the boost factor is determined by *D* and *M* is the modulation ratio. The output is influenced by the boost factor *B* (where ≥ 1), mirroring the traditional ZSI topology.

2.3. Comparative Study of Both ZSI Topologies

A comparative study was adopted between two Topologies in (Pavani, Venkatesh, et al 2017).

2.3.1. Voltage Stress and Ripple of Z-Capacitor

For both the traditional and improved ZSI topologies, the DC-link peak voltage, represented by V_i:

$$V_i = \frac{1}{1-2D} V_{pv} \tag{10}$$

Can be calculated using the duty ratio D in the shoot-through state according to during the shoot-through state, the voltage ripple of the Z-capacitor (ΔV_C) is determined by $\Delta V_C = \frac{I_L \ D \ (1-D)}{C}$. V_C is given in (7). In comparison, it is observed that V_C is decreased by V_{pv} while maintaining the same voltage boost. In traditional ZSI, topology V_C is given as:

$$V_{c1} = V_{c2} = V_c = \frac{1-D}{1-2D} \tag{11}$$

From (11), *Vc* is not less than V_{pv}, so voltage stress across Z-capacitor is high.

2.3.2. Current Ripple of Z-Inductor

The average current of the Z-inductor remains the same for both topologies and is equal to the average input current. The current ripple of the Z-inductor (Δi_L) is determined by different equations depending on the state:

- In IZSI when the non-shoot-through state. The current ripple is given as:

$$\Delta i_L = \frac{(1-D)TV_C}{L} \tag{12}$$

- In ZSI when the shoot-through state. The current ripple is given as:

$$\Delta i_L = \frac{DTV_C - D(1-D)TV_C}{L} \tag{13}$$

The ripple current remains consistent for both traditional and improved topologies.

2.3.3. Input Current Ripples

The input current (i_{in}) in the ZSI varies with control methods. For the traditional ZSI, $i_{in} = 2i_L - Ii$, where Ii is the inverter bridge current. In the shoot-through state, i_{in} is zero. At the beginning of the traditional ZSI, a huge inrush current occurs. The initial voltage of the Z-capacitors is zero, so the huge inrush current will charge the Z-capacitors immediately to 0.5 V_{pv} and starts the resonance at the Z-capacitors and the Z-inductors. This causes a large Z-inductor current and Z-capacitor voltage surge. In contrast, for the improved topology, the input current (i_{in}) is consistently $2i_L$ during the shoot-through state, simplifying analysis. The input current i_{in} averages to i_L for both traditional and improved topologies in active state.

3. The Improved Particle Swarm Optimization (IPSO) based MPPT

The efficiency of solar energy systems depends heavily on maintaining the maximum power point (MPP) of the photovoltaic (PV) module, which may fluctuate due to different weather conditions such as temperature and irradiance. To achieve optimal performance, implementing a maximum Power Point Tracking (MPPT) algorithm is essential. The MPPT algorithm continuously monitors the voltage and current of the solar panel and adjusts the operating parameters to maintain the MPP regardless of changes in sun angle and intensity. In this section, we propose an improved particle swarm optimization (IPSO) algorithm specifically tailored for MPPT applications.

3.1. Cuckoo search algorithm (CSA)

Cuckoo search is an optimization algorithm inspired by cuckoo birds' parasitic reproduction strategy. The optimization as MPPT function is discussed in (Mohamed, Osama abed el-Raouf et al 2019). CS Using the levy flights to update duty cycles values in terms of gamma function (γ) as equations in below (Abo-Elyousr, Farag K. et al 2019).

$$\delta = \left[\frac{\gamma(\beta+1)\times sin\pi \times \left(\frac{\beta}{2}\right)}{\gamma\left(\frac{\beta+1}{2}\right)\times\beta\times 2^{\frac{\beta-1}{2}}} \right]^{\frac{1}{\beta}} \tag{14}$$

$$x_i^{k+1} = x_i^k + \varepsilon\left(x_j^k - x_f^k\right) \tag{15}$$

Where:

u = uniformly distributed matrices of value 1,

v = uniformly distributed matrices of value δ.

In the searching mechanism of Cs based MPPT, begins by initializes the value of duty cycle D randomly between [0-1] and stores it in a matrix form. Thereafter, works to determine the Gbest value of D. If the system requires power to the load, the algorithm runs and removes the worst solutions and exchanges them with new nests.

3.2. Flower Pollination Algorithm (FPA)

The term pollination can be defined as the physiological process of plant mating. In general, there are two kinds of pollination namely self and cross-pollinate. Self-pollination happens when pollen of one flower fructifies the same flower or another flower in the same kind of plant. Whereas, cross-pollination occurs when grains of pollen is moved from various plants. Generally necessitates communicators such as birds, bees, and bats with levy flight characteristics (Jayaudhaya,Ramash Kumar et al., 2022). The flower pollination algorithm was firstly proposed by Yang et al., in 2012 (Shang, Zhu et al., 2018), and has been proved to be effective in searching for global optimal solutions within a short period. In recent years, it has been widely used to solve nonlinear optimization problems.

FPA can also be easily adjusted and has fewer parameters than other methods. The characterized equation for global pollination can be given as follows (Pei, Hao et al., 2018):

$$D_i^{k+1} = x_i^k + \gamma L(\lambda)\left(g_{\text{best}} - D_i^k\right) \tag{16}$$

$L(\lambda)$ is the Levy flight displacement corresponding to the flower individual, it is defined as:

$$L(\lambda) \approx \frac{\lambda\Gamma(\lambda)\times\sin\left(\frac{\pi\lambda}{2}\right)}{\pi} \times \frac{1}{S^{1+\lambda}} \text{ where}\left(s >> s_0 > 0\right) \tag{17}$$

Where λ is equivalent to 1.5; $\Gamma(\lambda)$ is a standard gamma function; S can be defined as:

$$S = \frac{\mu}{|\nu|^{1/\lambda}}, \tag{18}$$

Where μ and v obey normal distribution, $\mu \sim N(0,\sigma^2)$ and $v \sim N(0,1)$; σ^2 is defined as:

$$\sigma^2 = \left[\frac{\Gamma(1+\lambda)}{\lambda\Gamma\left((1+\lambda)/2\right)} \cdot \frac{\sin(\lambda\pi/2)}{2^{(\lambda-1)/2}} \right]^{\frac{1}{\lambda}} \tag{19}$$

The characteristic equation of local pollination can give as follows:

$$x_i^{k+1} = x_i^k + \varepsilon\left(x_j^k - x_f^k\right) \tag{20}$$

Where x_i^k is the i solution in the k iteration. x_j^k and x_f^k are randomly chosen pollen of the same type of plant from different flowers and ε is [0, 1].

The algorithm starts by initializing the duty cycle D randomly between [0-1] and storing it in a matrix. It then searches for the best value of D. During the operation of the system, the algorithm replaces the worst solutions with new nests to improve the search for the optimal value of D.

3.3. Traditional Particle Swarm Optimization (PSO)

Particle Swarm Optimization (PSO) algorithm, which is an intelligent optimization method inspired by the cooperative feeding behavior of birds. The PSO algorithm involves a population of particles, each representing a potential solution, moving around in the search space to find the best solution.

In the context of MPPT, the particle swarm position, and the fitness are taken as the duty cycle D and PV system output power respectively. The PSO algorithm utilizes mathematical formulas to update the positions and velocities of particles. The particle's position and velocity are updated based on (B Rezk, Hegazy, et al 2017):

$$D_i^{k+1} = D_i^k + v_i^{k+1} \tag{21}$$

Where V_i denotes step size at iteration k+1

$$v_i^{k+1} = wv_i^k + c_1 r_1 \left(P_{best} - d_i^k \right) + c_2 r_2 \left(G_{\text{best}} - D_i^k \right) \tag{22}$$

Where w denotes inertial weight, c1, and c2 denote the acceleration coefficients r1, and r2 random values. Pbest denotes the best position of a particle i and Gbest denotes the best position in the entire population. The inertial weight w is defined as 0.1, the personal learning coefficient c1 is set at 1.2, the global learning coefficient c2 is set at 1.7 and the minimum and maximum velocity Vi of the particles are fixed at [-0.07 0.072].

3.4. Limitations of Traditional PSO for MPPT

While traditional PSO performs well in various optimization tasks, it has some limitations when applied to MPPT for PV systems. These limitations include:

- ✓ Low Accuracy: Traditional PSO may exhibit low accuracy in rapidly changing environmental conditions, especially under varying irradiance levels. This can lead to suboptimal power generation and reduced efficiency.
- ✓ Slow Convergence: Traditional PSO may converge slowly to the MPP, particularly when the PV system operates at Standard Test Conditions (STC) or faces challenging environmental changes.

3.5. The Proposed Improved Particle Swarm Optimization (IPSO)

The IPSO algorithm introduces modifications to traditional PSO to enhance the efficiency and accuracy of Maximum Power Point Tracking (MPPT) in photovoltaic (PV) systems. To achieve this, the particle swarm is divided into several groups, facilitating better exploration and convergence to local optima. The following steps, as presented by (Yang, Zengrui et al., in 2017), were employed to develop and demonstrate the Improved PSO (IPSO) algorithm. These steps involve dividing the particle swarm into groups and adjusting the updated formulas and tactics of PSO accordingly.

(a) In each group, The global best value updated by the particle's position and speed for the best particles of groups, and the formulas are stated as:

$$V_n^{k+1} = \omega V_n^k + c_1 r_1 \left(P_m^k - X_n^k \right) \tag{23}$$

$$\mathrm{D_n^{k+1}} = \mathrm{D_n^k} + \mathrm{V_n^{k+1}} \tag{24}$$

Where Pm is the best position of particles in the mth group, m=1, 2, M, M is the number of groups, and n=1, 2, N-1, N is the number of particles within group.

(b) he global best value updated by the particle's position and speed for the best particles of groups and the formulas are stated as:

$$V_n^{k+1} = c_2 r_2 \left(P_g^k - D_m^k \right) \tag{25}$$

$$P_n^{k+1} = P_n^k + V_n^{k+1} \tag{26}$$

Where Pg represents the optimal position of all the swarm's particles. The (Pr-Pm) in eq (26) is zero in the iterative approach when the group's best values are equal to the overall best value. The particle will remain unaltered as a result. A minor perturbation constant is permitted to be added in to prevent this from happening (10).

The flowchart representing the IPSO method for MPP tracking is shown in Figure 5.

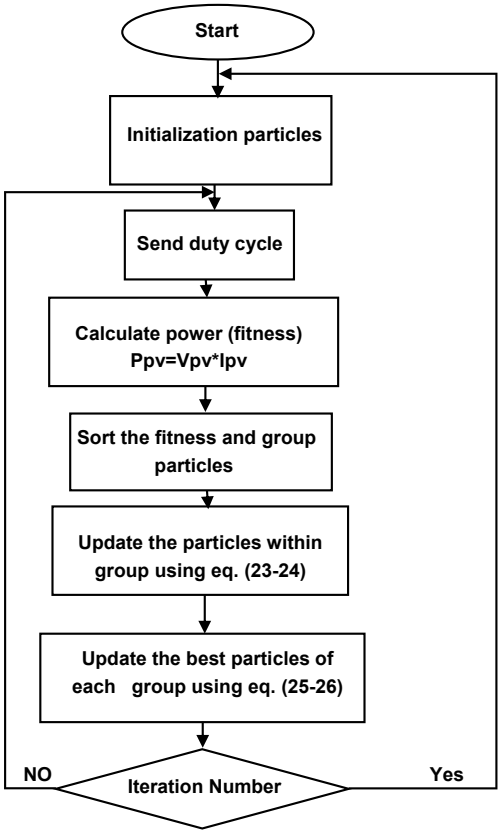

Fig. 5. Flowchart of IPSO algorithm.

4. The Improved Z-Source Inverter Control Strategies

There are numerous control schemes available for the three-phase inverter with a z-source structure, each with benefits and drawbacks as well as appropriate application areas. Generally, in traditional inverter there are various conventional PWM techniques like Sine triangle PWM, and Space Vector PWM techniques. Likewise, in Z-source inverters there are various types of conventional PWM techniques used to control Z-source inverters is the same control in the proposed Z-source inverter. These techniques are Simple Boost Control (SBC), Maximum Boost Control (MBC) Maximum Boost Control with third harmonic injection. The general principle of these strategies are based on the addition of two additional reference signals. Intended for the generation of the short-circuit state, to get the higher output voltage.

4.1. Simple Boost Control (SBC) of the Improved Z-Source Inverter

Aspired by (Suganthi, J. and M. Rajaram 2015) This technique produces switching pulses by comparing three modulating signals (Va for A-phase, Vb for B-phase, and Vc for c-phase) with a 120-degree phase shift when compared with high frequency carrier triangular signal. When two straight dc lines are compared to the carrier signal, the shoot-through for the Z-source inverter is produced. These dc lines' magnitudes, Vp and Vn (where Vp=-Vn), Shoot-through pulses are produced when the carrier signal is higher than Vp and less than Vn. Shoot-through duty ratio D=T0/T. Where the carrier period T and the time length for shoot-through T0. Actual switching pulses for the Z-source inverter are now OR between the traditional switching pulses depicted in the following Figure 6.

The relationship between these two parameters are expressed by the following equations:

$$D = 1 - M \tag{27}$$

$$B = \frac{1}{1 - 2\frac{T_0}{T}} = \frac{1}{1 - 2D} = \frac{1}{1 - 2(1 - M)} = \frac{1}{2M - 1} \tag{28}$$

$$\mathrm{G} = \mathrm{M.B} = \frac{\mathrm{M}}{2\mathrm{M} - 1} \tag{29}$$

Where G is inverter voltage gain, M is modulation index and B is boost factor. The peak phase voltage of the Z-source inverter is given by:

$$V_{ac} = M \cdot B\frac{V_{Pv}}{2} \tag{30}$$

In Figure 7, the high frequency carrier signal is used to compare the sinusoidal signals of each phase, V_a, V_b and V_c. The shoot-through that is produced is then OR gated with the pulse generator's output by compare the carrier signal with V_p and V_n, allowing us to acquire the modified signal with the shoot-through injection.

4.2. Maximum Constant Boost Control with Third Harmonic Injection (THIMCBC) for the Improved Z-Source Inverter

For both a stand-alone load and a system that is connected to the grid, the use of constant boost control with traditional dc power sources has been examined (Khajesalehi, J., Sheshyekani, K., Hamzeh, M., et al 2016) Three-phase inverter systems frequently use thethird harmonic injection. The thumbnail map is displayed in Figure 8. Suppose modulated wave of phase A is expressed as (Zhao, Zhengyu et al., 2019).

$$v_a = M\sin(\theta) \tag{31}$$

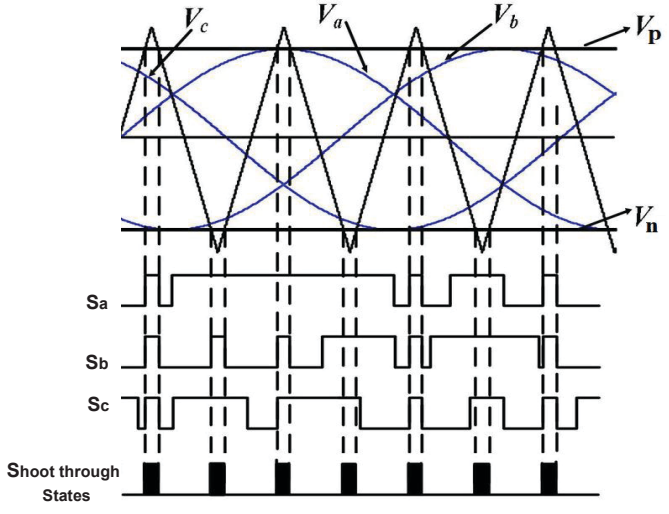

Fig. 6. PWM Signals from Simple Boost control.

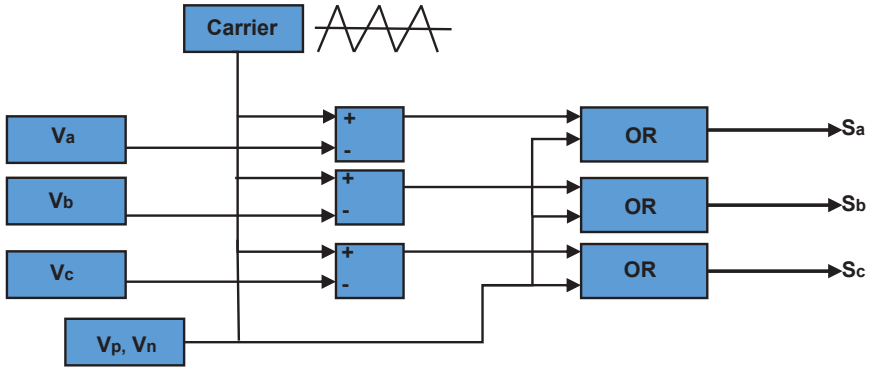

Fig. 7. Bloc diagram of PWM generating signals using SBC method.

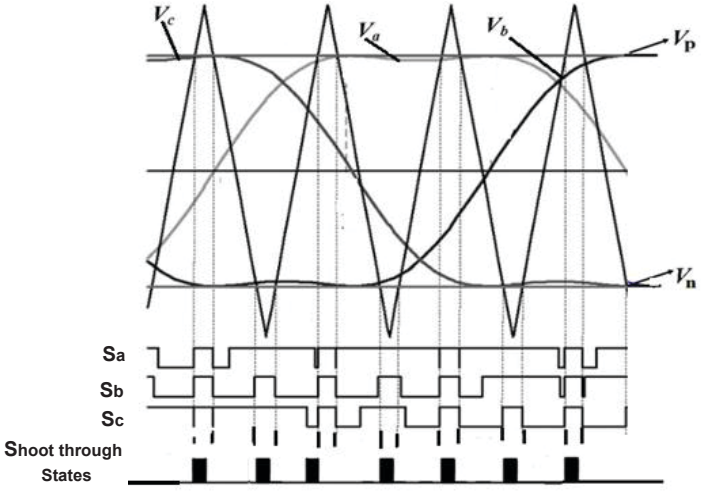

Fig. 8. Sketch map of constant boost control with third harmonic injection.

When the third harmonic is injected, it could be expressed as:

$$v_a' = M\sin(\theta) + aM\sin(3\theta) \tag{32}$$

Then, for this control, in a method the modulation index can be increased from1 to 2/√3 and the maximum shoot through duty ratio is limited to (1-√3/2 M). For any desired modulation index M, the obtainable maximum voltage gain is:

$$G = MB = \frac{M}{\sqrt{3}M - 1} \tag{33}$$

In addition, for any desired voltage gain G, the maximum modulation index can be used is:

$$M = \frac{G}{\sqrt{3}G - 1} \tag{34}$$

5. PV System with improved Z-source inverter

An MPPT-based IPSO has been proposed to operate a PV panel at its maximum power output. The IPSO modifies the duty ratio based on the PV parameters such as voltage and current to operate at the maximum power point,

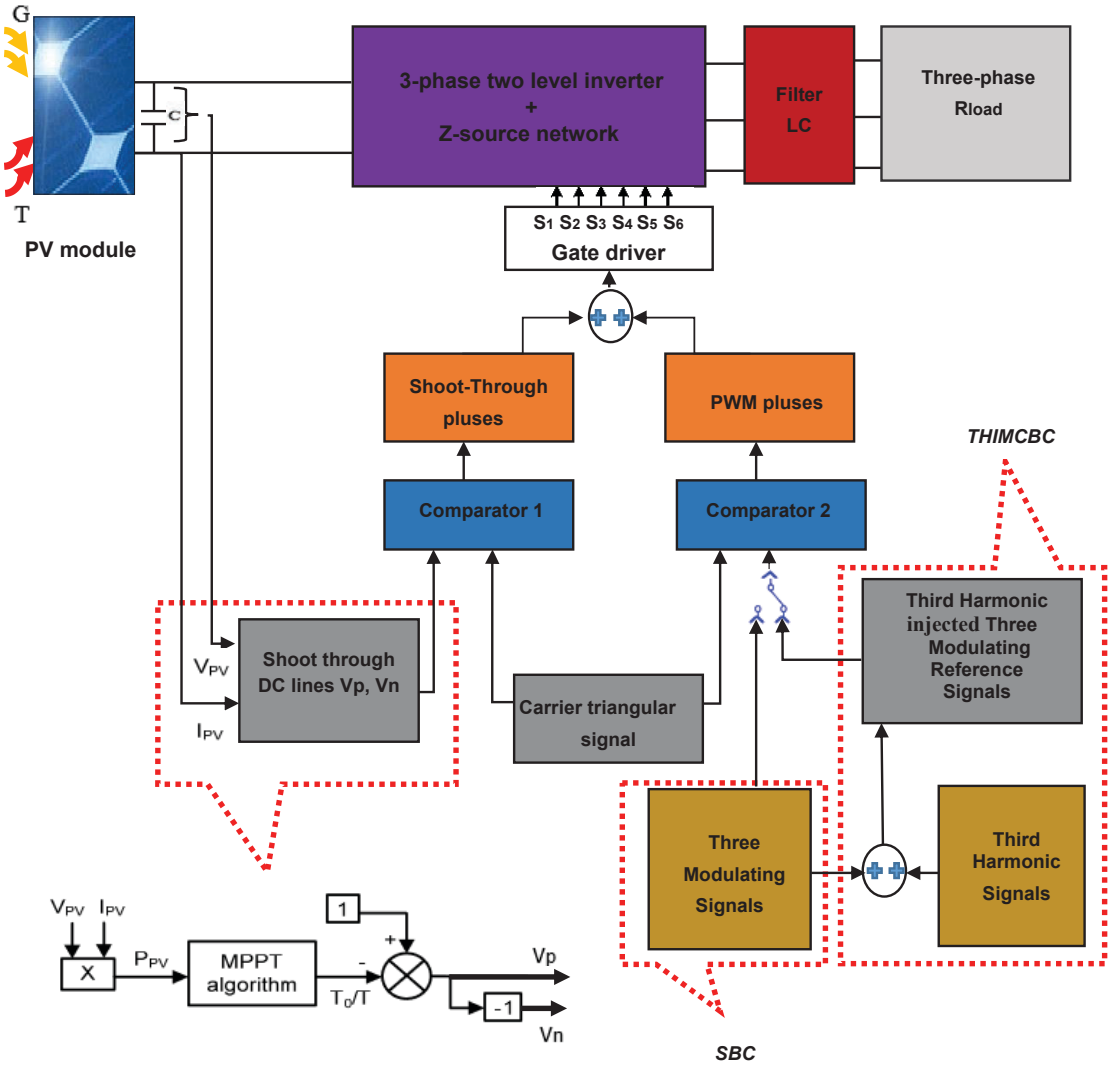

Fig. 9. Block diagram of the PV- improved Z-Source inverter.

which varies depending on the atmospheric conditions and load characteristics. The inverter's boost operation is achieved using the shoot-through time period concept, with the MPPT program controlling the shoot-through duty cycle. The Pulse Width Modulation (PWM) signals are used to control the active and zero states, with sinusoidal signals compared to a triangular signal. The third harmonic injection technique is used in THIMCBC to inject three modulating reference signals, while in SBC only sinusoidal signals are used as reference as show in Figure 9.

The third harmonic injection technique extends the boost range of the converter, enabling it to step up the output voltage even when the input voltage is very low.

6. Simulation and Results

MATLAB/SIMULINK® software was used to simulate the MPPT-based control, and two controllers are provided based on the control strategy of an improved Z-source inverter. The configuration for the MATLAB software solver was adjusted to run the algorithm with a fixed step size of 5 seconds. The simulation results were obtained based on the parameters: input voltage Vpv=70V, load: three-phase resistance Rload = 50, Z source network: L1=L2=5mH C1=C2==C=1500μF, output filter: Lf=15mH, Cf= 10μFand carrier wave frequency = 10 KHz.

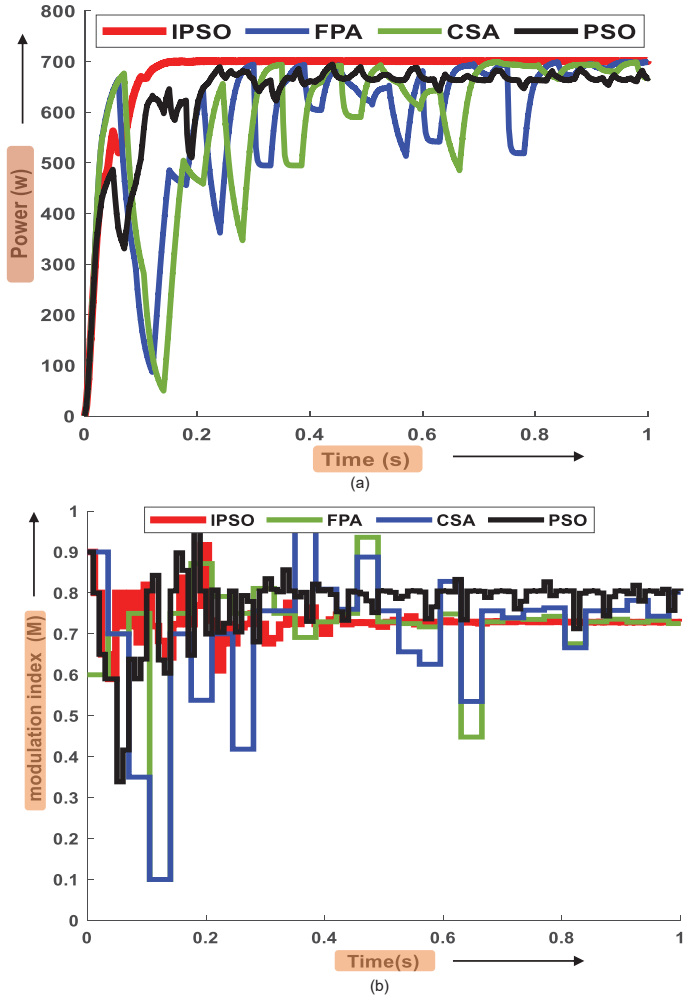

Fig. 10. (a) Tracking process of MPP (Ppv) under STC. (b) Modulation index (M).

In the initial analysis, both Particle swarm optimization (PSO), Cuckoo Search Algorithm (CSA), as well as Flower Pollination Algorithm (FPA) and Improved Particle Swarm Optimization (IPSO) MPPT methods were evaluated under Standard Test Conditions (STC) in Figure 10. Additionally, a comparative assessment of these MPPT methods was conducted under varying sunlight levels in Figure 11.

6.1. Output Power Performance under Constant Irradiance

In STC (25°C and 1000W/m^2), The PV model used in this paper has the 700 Watt peak for optimal power. The performance results of both MPPT are shown in Figure 10 (a).

Several crucial metrics were examined in the evaluation of Maximum PowerPoint Tracking (MPPT) approaches to judge their effectiveness. Included in this were the following: Rated Power (W), Tracking Time (s), Tracking Efficiency (%), and Power Fluctuations. The PSO method achieved a tracking efficiency of 94.62% with a tracking time of 0.95 seconds, extracting 662.8 W of power from the PV output of 700 W. It showed relatively high power fluctuations. In contrast, the CSA approach demonstrated a slightly improved tracking effectiveness of 97.17% within a shorter tracking time of 0.85 seconds and produced a power extraction of 680.2 W, slightly higher than PSO. It did, however, also exhibit noticeable power variations. In the Flower Pollination Algorithm (FPA) method, power extraction reached 689.9 W, displaying an impressive tracking efficiency of 98.55% within a tracking time of 0.82 seconds. However, akin to the previous methods, it also encountered high power fluctuations. Notably, the Improved Particle Swarm Optimization (IPSO) method exhibited exceptional performance by achieving a perfect

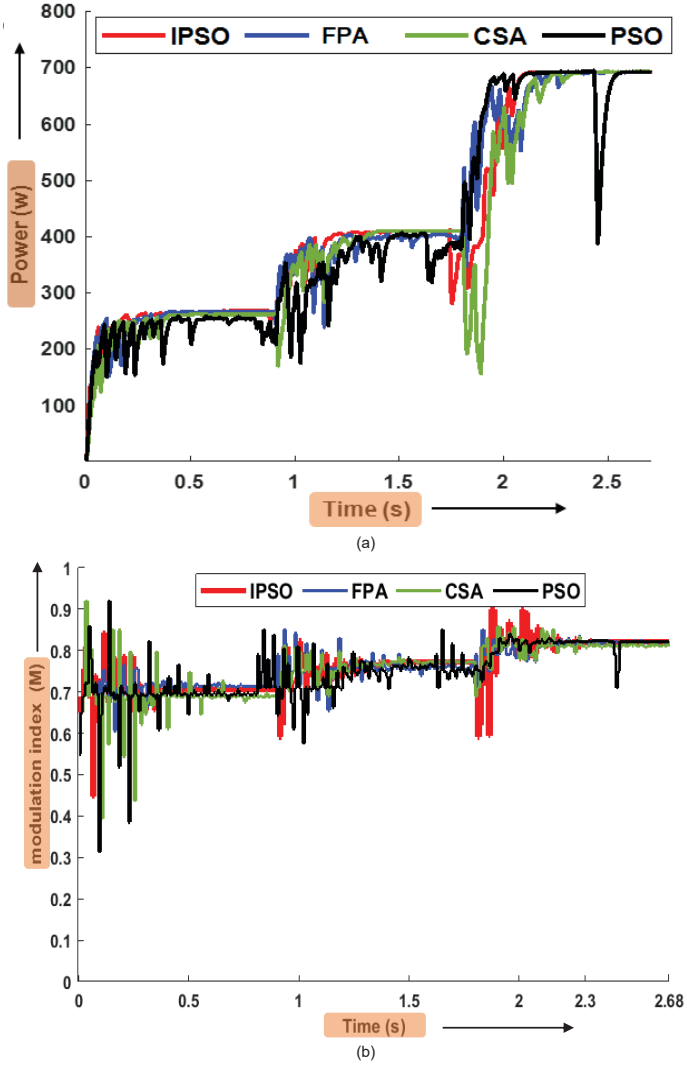

Fig. 11. (a) Tracking process of MPP (Ppv) under varying irradiance. (b) Modulation index (M).

tracking efficiency of 100%. It successfully extracted the maximum power of 700 W from the PV system within an astonishingly short tracking time of 0.1 seconds, with power fluctuations being very small.

Figure 10 (b) illustrates the MPPT-based iteration method for changing the modulation index (M) of the improved Z-source inverter (IZSI). The PSO method is shown as a black line with an initial M value of 0.9. The iterative approach resulted in an M value that varied between 0.69 and 0.82. The iteration process for the CSA method, represented by the green line, began with an initial M value of 0.9. There was a delayed iterative process, converged after 0.85 seconds and then stabilized in M=0.71. The blue line in this graph shows the same results for FPA. The initial values of M are set to 0.9 for the IPSO approach, which is represented by the red line. It showed a fast iteration cycle that converged and reached stability 0.4 seconds ago.

6.2. Output Power Performance under Varying Irradiance

Performance evaluation requires a thorough understanding of the important interaction between illumination and photovoltaic (PV) system power production. PV system power production increases as illumination does, demonstrating the system's sensitivity to light level. Under varying irradiance, it is crucial to optimize MPPT algorithms for PV output power because illumination reflects incident light intensity on the surface of the PV panel. We purposefully changed the radiation levels used to test the Maximum Power Point Tracking (MPPT) algorithms

in order to simulate real-world settings. Intended to test MPPT algorithms, Different radiation was applied to a solar panel as follows:

- From Time = (0 to 1) s. G=400W/m^2 and 25^{0}C. P_{PV}= 272W.
- From Time = (1 to 2) s. G=600W/m^2 and 25^{0}C. P_{PV}= 410W.
- From Time = (2 to 3) s. G=1000W/m^2 and 25^{0}C. P_{PV}= 700W.

The dynamic tracking of the Maximum Power Point (MPP) with variable irradiance is depicted in Figure 11(a). The maximum energy point exhibits a noticeable fluctuation when the Particle Swarm Optimization (PSO) algorithm is applied. At various radiation levels, there is a sizable energy loss and delay in reaching the maximum energy point. However, when the Cuckoo Search Algorithm (CSA) and the Flower Pollination Algorithm (FPA) are applied, a significant improvement is seen, leading to a significant reduction in oscillations and a faster convergence to the point of maximum energy. Additionally, IPSO exhibits amazing stability and great performance at the point of maximum energy for each radiation intensity. A considerable improvement in convergence speed for quick and accurate monitoring of the point of maximum energy across different radiation conditions.

With an optimal power of 272 W in G=400W/m^2 and 25^{0}C, the Particle Swarm Optimization (PSO) method produces roughly 250 W from the photovoltaic (PV) system and a tracking efficiency of 91.91%. The Cuckoo Search Algorithm (CSA) generates about 248.96 W from the PV system, with a slightly higher power of 260.3 W and a tracking efficiency of 95.58%. It is noteworthy that the Flower Pollination Algorithm (FPA) method with a nominal power of 264.62 W achieves a parallel power output from the PV system of the same order of magnitude. Its tracking efficiency of 97.28% ensures efficient conversion of solar energy with moderate power fluctuations. Finally, the improved particle swarm optimization (IPSO) method has a PV power of 271.9 W, which offers an impressive tracking efficiency of 99.96% and minimal power fluctuations very small.

In the specific solar conditions of G=600W/m2 and a temperature of 25°C, the photovoltaic (PV) system displayed a power output, peaking at an impressive 410 W. The investigation into different optimization methods further highlighted their impact on the system's performance. The Particle Swarm Optimization (PSO) exhibited a power output of 389.3 W, with a tracking efficiency of 94.95%. However, it also showed a drawback with relatively high power fluctuations. On the other hand, the Cuckoo Search Algorithm (CSA) achieved a slightly higher power output of 391 W and a tracking efficiency of 95.36%, displaying moderate power fluctuations. The Flower Pollination Algorithm (FPA) and the Improved Particle Swarm Optimization (IPSO) stood out with power outputs of 397.1 W and 409 W, respectively. FPA displayed a tracking efficiency of 96.85% with moderate power fluctuations, while IPSO boasted an impressive tracking efficiency of 99.75% and minimal power fluctuations. Under solar conditions G = 1000 W/m2 and a temperature of 25 °C, the same results are observed with constant irradiation. These results strongly suggest that IPSOs have potential for highly efficient power generation under a range of specified and varied environmental conditions. It highlights the crucial role of IPSO as a suitable algorithm choice and demonstrates its ability to not only maximize power output but also optimize efficiency in the ever-changing dynamics of different solar environments. Choosing IPSO can therefore be a strategic step to ensure consistent and effective solar energy use, ultimately contributing to a more sustainable energy landscape.

In Figure 11 (b), we examine the MPPT-based iteration method and illustrate how we adjust the modulation index (M) for the IZSI under different irradiance conditions. The PSO method started with an initial M value of 0.5, which resulted in a varying M value during the iteration process. Conversely, the CSA method started with an initial M value of 0.65, resulting in a delayed iterative process that eventually stabilized after a longer duration under varying radiation. On the other hand, starting from initial M values of 0.68, the FPA method showed a fast iteration cycle that successfully converged and achieved stability, slightly outperforming the PSO and CSA approaches in terms of speed. However, there was a slight delay in convergence. Finally, the IPSO approach started with an initial M value of 0.68 and showed a fast iteration cycle that converged quickly, making it the optimal choice for achieving stability and rapid response under fluctuating radiation levels.

6.3. Reduction of Inrush Current and Capacitor Stress

The simulation results of the traditional and improved topologies, respectively, when the results were obtained using IPSO as MPPT and THIMCBC. Under T= 25 °C and G=1000 W/m^2. The PV model used in this study has an optimal power of 700 watts and an optimal power voltage of 70 V with duty cycle D=0.29 and modulation index M=0.71.

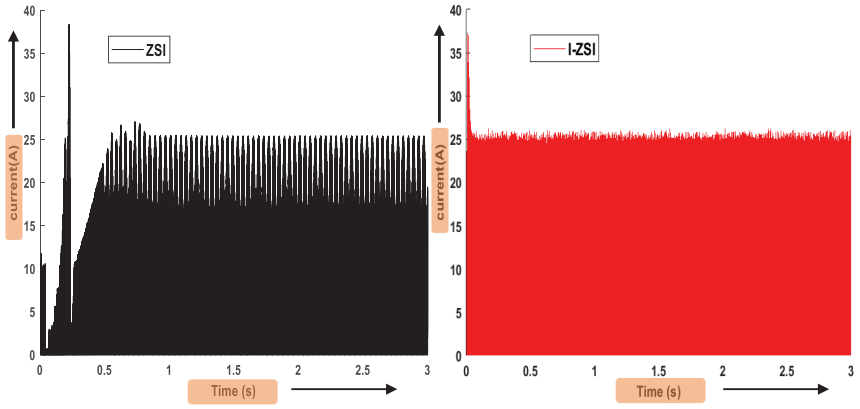

(a)

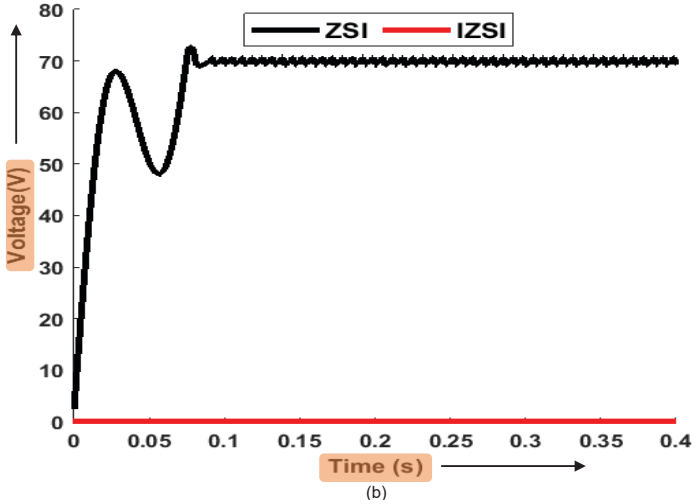

(b)

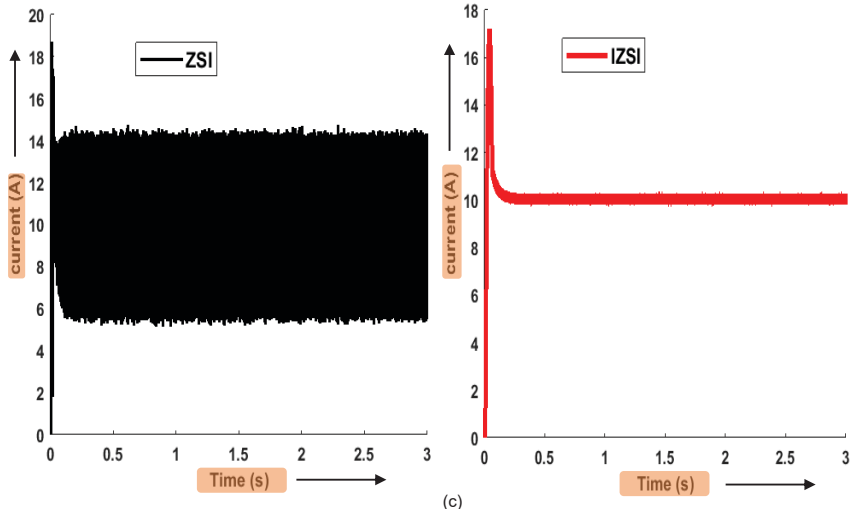

(c)

Fig. 12. Output waveforms of traditional and improved topologies. (a) The inverter bridge current Ii. (b) Z-capacitor Vc. (c) Current of Z-inverter IL1.

Figure 12 show the waveforms from top to bottom are the inverter bridge current Ii, Z-capacitor voltage VC, Z-inductor current IL, respectively. We can see that in the traditional topology, VC is equal to Vpv =70 V in steady state and a huge inrush current occurs at start-up. Then the resonance between the Z-capacitors and Z-inductors

starts, and the voltage and current surges occur. This may destroy the converter. Simulation results under improved topology, the inrush current is avoided at start-up, VC is equal to 0 in steady state, and the resonance between the Z-capacitors and Z-inductors can be neglected. Thus, the system security can be guaranteed.

6.4. The control strategy employed in the IZSI for boosting Vpv

The control strategy employed in the Improved Z-Source Inverter (IZSI) for boosting the voltage from the photovoltaic source (Vpv) involves managing the modulation index and duty cycle to regulate the output voltage and ensure efficient power conversion. This control mechanism allows for precise adjustment and optimal utilization of the boosted voltage for specific application requirement. The results were obtained using IPSO as MPPT under constant irradiation at standard test conditions (STC) of 25 °C and 1000 W/m. The PV model used in this study has an optimal power of 700 watts and an optimal power voltage of 70 V with duty cycle D=0.29 and modulation index M=0.71.

In Figures 13 and 14, show the Van voltage of the IZSI before and after the LC filter using the Inertia Weight Particle Swarm Optimization (IPSO-MPPT) technique along with two control methods: SBC and THIMCBC for the IZSI under STD. The figures illustrate the output voltage and a comparison of two control strategies, SBC and THIMCBC, for an enhanced Z-source inverter (ZSI) integrated with an LC filter and exposed to a balanced three-phase load of 50. The THIMCBC strategy has higher efficiency, resulting in the inverter's DC link voltage (Vpv)

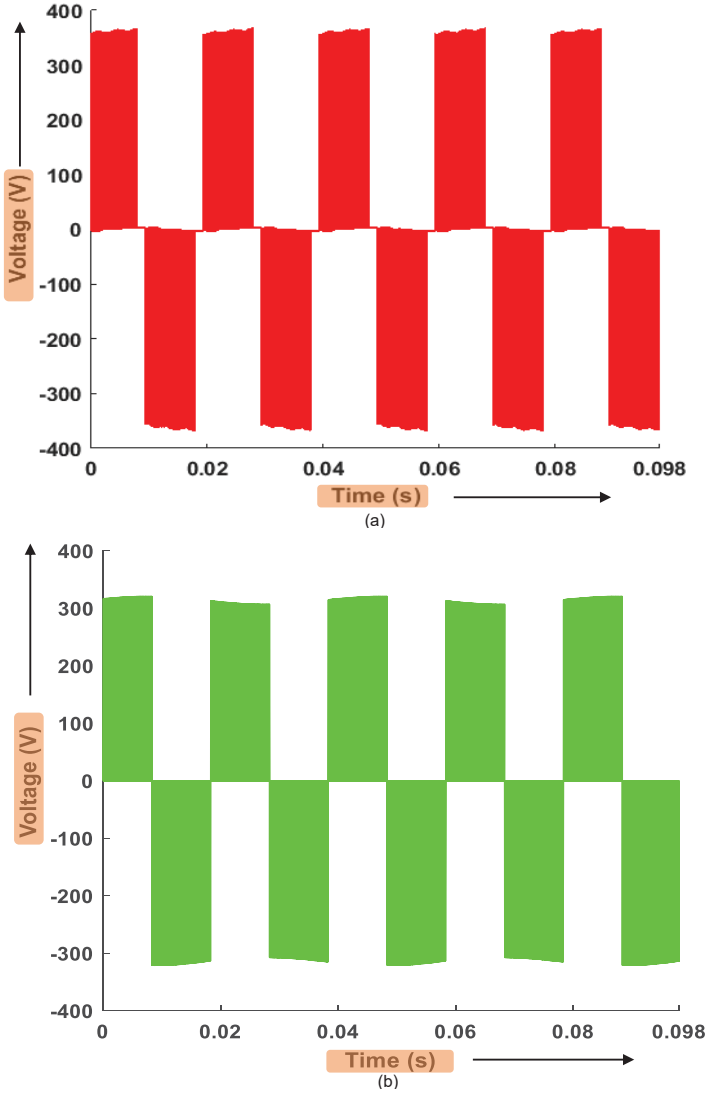

Fig. 13. Voltage performances of improved ZSI (Va). (a) THIMCBC: Red. (b) SBC: green.

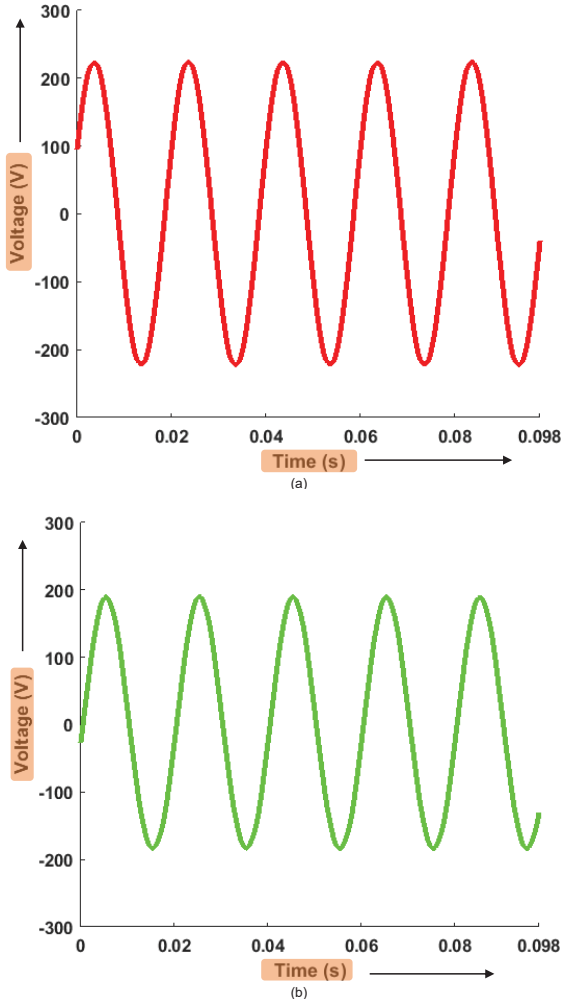

Fig. 14. Voltage performances of improved ZSI using LC filter (Van). (a) THIMCBC: Red. (b) SBC: green.

increasing to 367.2 V (B=5.26), compared to SBC where Vpv increases to 345V (B=4.7). In addition, the peak voltage waveforms of the output line after the LC filter of the improved ZSI with the THIMCBC method reach up to 220V more than the peak voltage sine waveforms of the output line of the improved ZSI with the SBC method, which reach values below 180V.

7. Conclusion

To improve the performance of the Z-source inverter (ZSI) in photovoltaic systems, this paper provides. Improved Z-Source Inverter (ZSI) that offers a number of advantages over traditional ZSI. This offers advantages such as lower voltage loading on the Z-source capacitor and integrated inrush current limitation. It is noteworthy that this further development corresponds to the classic Z-source inverters (ZSI) in terms of financial aspects and control strategies. The study includes a comparative analysis of several Maximum Power Point Tracking (MPPT) methods such as : PSO, CSA, FPA and Improved Particle Swarm Optimization (IPSO). The clear results show that IPSO is the optimal choice for improved ZSI applications compared to traditional algorithms. Furthermore, this study provides a comparative analysis of two different control strategies: SBC and the THIMCBC method. In particular, the THIMCBC approach shows a remarkable boost effect, denoted by factor B, showing a significant performance increase of the improved Z-source inverter (IZSI). Contributes significantly to the overall improvement of ZSI performance and results in a boosting voltage Vpv.

References

Peng, B., Ho, K., and Liu, Y. (2018). A Novel and Fast MPPT Method Suitable for Both Fast Changing and Partially Shaded Conditions. *IEEE Transactions on Industrial Electronics, 65*, pp. 3240-3251.

Jayaudhaya, J., Ramash Kumar, K., Tamil Selvi, V., & Padmavathi, N. (2022). Improved Performance Analysis of PV Array Model Using Flower Pollination Algorithm and Gray Wolf Optimization Algorithm. *Mathematical Problems in Engineering*. doi: 10.1155/2022/5803771.

Ali, A.I. and Mohamed, H.R. (2022). Improved P&O MPPT algorithm with efficient open-circuit voltage estimation for two-stage grid-integrated PV system under realistic solar radiation. *International Journal of Electrical Power & Energy Systems*. doi: 10.1016/j.ijepes.2021.107805.

Anto, E.K., Okyere, P.Y., & Asumadu, J.A. (2014). Critical voltage perturbation size for an open loop perturb and observe (P&O) maximum power point tracking (MPPT) grid-connected solar photovoltaic (PV) system. *2014 IEEE 40th Photovoltaic Specialist Conference (PVSC)*, pp. 1912-1916.

Balasubramanian, A.K., Ramachandran, S. and Shanmugavelu, S. (2022). Effectual GA Optimized PID Control Strategy based MPPT Controller for Extracting Maximum Power from Photo Voltaic system. *Trends in Sciences, 19*(9), 3969. doi: 10.48048/tis.2022.3969.

Mahapatra, S and Sah, C.K. (2021). Novel Hybrid GWO–IC Based MPPT Technique for PV System under Partial Shading Conditions. *Proceedings of the ISES Solar World Congress 2021*. doi :10.1038/s41598-022-14733-6.

Tey, K.S., Mekhilef, S. and Seyedmahmoudian, M. (2018). Implementation of BAT Algorithm as Maximum Power Point Tracking Technique for Photovoltaic System under Partial Shading Conditions. *2018 IEEE Energy Conversion Congress and Exposition (ECCE)*, pp. 2531-2535.

Chauhan, U., Chhabra, H., Rani, A., Kumar, B. and Singh, V. (2022). Efficient MPPT Controller for Solar PV System Using GWO-CS Optimized Fuzzy Logic Control and Conventional Incremental Conductance Technique. *Iranian Journal of Science and Technology, Transactions of Electrical Engineering,* pp. 463-472.

Luthfansyah, M., Suyanto, S. and Bangura, A.B. (2020). Evaluation and Comparison of DC-DC Power Converter Variations in Solar Panel Systems Using Maximum Power Point Tracking (MPPT) Flower Pollination Algorithm (FPA) Control. *E3S Web of Conferences*. doi :10.1051/e3sconf/202019000026.

Hanafiah, S., Ayad, A., Hehn, A. and Kennel, R. (2017). A hybrid MPPT for quasi-Z-source inverters in PV applications under partial shading condition. *2017 11th IEEE International Conference on Compatibility, Power Electronics and Power Engineering (CPE-POWERENG)*. pp. 418-423, doi: 10.1109/CPE.2017.7915208.

Subhani, N., Kannan, R., Mahmud, A. and Blaabjerg, F. (2021). Z-source inverter topologies with switched Z-impedance networks: A review. *IET Power Electronics*. pp. 727-750. doi:10.1049/pel2.12064.

Jamal I., Elmorshedy M. F., S. M. Dabour, E. M. Rashad, W. Xu and D. J. Almakhles. (2022). A Comprehensive Review of Grid-Connected PV Systems Based on Impedance Source Inverter. In *IEEE Access*, pp. 89101-89123, doi: 10.1109/ACCESS.2022.3200681.

Amudhavalli, D. and Narendran, L. (2012). Speed control of an induction motor by V/F method using an improved Z source inverter. *2012 International Conference on Emerging Trends in Electrical Engineering and Energy Management (ICETEEEM)*, pp. 436-440. doi: 10.1109/ICETEEEM.2012.6494486.

Jamal, I., Elmorshedy, M.F., Dabour, S.M., Rashad, E.E., Xu, W. and Almakhles, D.J. (2022). A Comprehensive Review of Grid-Connected PV Systems Based on Impedance Source Inverter. *IEEE Access,* pp. 89101-89123.

Hayder, W., Ogliari, E.G., Dolara, A., Abid, A., Ben Hamed, M. and Sbita, L. (2020). Improved PSO: A Comparative Study in MPPT Algorithm for PV System Control under Partial Shading Conditions. *Energies,* 13(8). doi :10.3390/en13082035.

Ibtissam, C., Madjid, B.E. and Paul, G.J. (2018). Study of Fuzzy Logic controller based MPPT and the P&O for the Z-source inverter integrated in PV system. *2018 International Conference on Electrical Sciences and Technologies in Maghreb (CISTEM)*, pp. 1-6.

Jagan, V. and Das, S. (2015). High boosting type Z-source inverter improved Z-source inverter for solar photovoltaic system. *2015 Annual IEEE India Conference (INDICON)*, pp.1-6.

Yu, K., Luo, F.L., and Zhu, M. (2010). Study of an improved Z-source inverter: Small signal analysis. *2010 5th IEEE Conference on Industrial Electronics and Applications*, pp. 2169-2174.

Tang, Y., Xie, S., & Zhang, C. (2011). An Improved Z-Source Inverter. *IEEE Transactions on Power*

Electronics, pp. 3865-3868. doi:10.1109/TPEL.2009.2039953.

Pavani, B., Venkatesh, K., & Sekhar, P.C. (2017). An Improved Z-Source Inverter for Reduction in Inrush Current and Stress on Capacitor. *SSRG International Journal of Electrical and Electronics Engineering (SSRG-IJEEE)*. 4(7). pp. 27-30. doi: 10.14445/23488379/IJEEE-V4I7P106.

Mosaad, M.I., abed el-Raouf, M., AL-AHMAR, M.A., and Banakher, F.A. (2019). Maximum Power Point Tracking of PV system Based Cuckoo Search Algorithm; review and comparison. *Energy Procedia*. pp. 117-126. doi:10.1016/j.egypro.2019.04.013.

Abo-Elyousr, F.K., Abdelshafy, A.M. and Abdelaziz, A.Y. (2019). MPPT-Based Particle Swarm and Cuckoo Search Algorithms for PV Systems. *Modern Maximum Power Point Tracking Techniques for Photovoltaic Energy Systems*. doi: 10.1007/978-3-030-05578-3_14.

Jayaudhaya, J., Ramash Kumar, K., Tamil Selvi, V. and Padmavathi, N. (2022). Improved Performance Analysis of PV Array Model Using Flower Pollination Algorithm and Gray Wolf Optimization Algorithm. *Mathematical Problems in Engineering*. doi:10.1155/2022/5803771.

Shang, L., Zhu, W., Li, P. and Guo, H. (2018). Maximum power point tracking of PV system under partial shading conditions through flower pollination algorithm. *Protection and Control of Modern Power Systems,* pp. 1-7.

Pei, T., Hao, X., & Gu, Q.J. (2018). A Novel Global Maximum Power Point Tracking Strategy Based on Modified Flower Pollination Algorithm for Photovoltaic Systems under Non-Uniform Irradiation and Temperature Conditions. *Energies*. 11(10). doi:10.3390/en11102708.

Rezk, H., Fathy, A., & Abdelaziz, A.Y. (2017). A comparison of different global MPPT techniques based on meta-heuristic algorithms for photovoltaic system subjected to partial shading conditions. *Renewable & Sustainable Energy Reviews,* pp. 377-386.

Yang, Z., Duan, Q., Zhong, J., Mao, M and Xun, Z. (2017). Analysis of improved PSO and perturb & observe global MPPT algorithm for PV array under partial shading condition. *2017 29th Chinese Control and Decision Conference (CCDC)*, pp. 549-553.

Suganthi, J., & Rajaram, M. (2015). Effective analysis and comparison of Impedance Source Inverter topologies with different control strategies for Power Conditioning System. *Renewable & Sustainable Energy Reviews,* pp. 821-829.

Khajesalehi, J., Sheshyekani, K., Hamzeh, M and Afjei, E. (2016). Maximum constant boost approach for controlling quasi-Z-source-based interlinking converters in hybrid AC–DC microgrids. *IET Generation Transmission & Distribution, 10(4)*, pp. 938-948.

Zhao, Z., Elgendy, M.A., Armstrong, M. and Muhammad, M. (2019). Constant Boost Control with Third Harmonic Injection for Quasi-Z Source Inverter used in PV Grid-connected System. *2019 21st European Conference on Power Electronics and Applications (EPE '19 ECCE Europe)*, doi: 10.23919/EPE.2019.8915379.